Inhibition of Sclerostin by Systemic Treatment with Sclerostin Antibody Enhances Healing of Proximal Tibial Defects in Ovariectomized Rats

Michelle M. McDonald,[1] Alyson Morse,[1] Kathy Mikulec,[1] Lauren Peacock,[1] Nicole Yu,[1] Paul A. Baldock,[2] Oliver Birke,[1] Min Liu,[3] Hua Zhu Ke,[3] David G. Little[1]

[1]The Children's Hospital, Locked Bag 4001, Westmead, New South Wales 2145, Australia, [2]The Garvan Institute of Medical Research, Sydney, Australia, [3]Amgen Inc., Thousand Oaks, California

Received 14 July 2011; accepted 23 February 2012
Published online 27 March 2012 in Wiley Online Library (wileyonlinelibrary.com). DOI 10.1002/jor.22109

ABSTRACT: Recent studies suggest a possible role for inhibitors of sclerostin such as sclerostin antibody (Scl-Ab) as an anabolic treatment for osteoporosis. Since Scl-Ab has also been shown to potentiate bone repair, we examined the effect of Scl-Ab treatment in a metaphyseal defect repair model in ovariectomized (OVX) rats. Four weeks after OVX or sham surgery, 3 mm circular defects were created bilaterally in the proximal tibia of all rats. After defect surgery, Saline or 25 mg/kg Scl-Ab was administered twice weekly for 3 weeks. Of note, healing was advanced in the 1-week post-defect surgery in OVX controls over Sham controls, with increases in bone volume and fluorochrome labeling observed. However, by week 2, OVX controls fell significantly behind in the repair response compared with Sham controls. Scl-Ab treatment significantly increased bone volume in the defect in OVX rats over the 3-week time course as examined by either microCT or histology. Significant increases in bone formation via fluorochrome labeling of the new bone were observed with Scl-Ab treatment, while osteoclast parameters were not different. With its powerful anabolic potential, bone-specific activity, and potential for low dosing frequency, Scl-Ab treatment could provide enhanced bone repair, particularly in situations of compromised bone repair such as osteoporotic bone. J Orthop Res 30:1541–1548, 2012

Keywords: sclerostin; bone; defect; repair; formation

Sclerostin is a negative regulator of bone formation which was discovered through the detection of a mutation in the *SOST* gene in patients diagnosed with the high bone mass disease, sclerosteosis.[1] Parallel to the human disease, mice with a targeted deletion of *SOST* demonstrate an extremely high bone mass phenotype, highlighting the conservation of sclerostin's negative regulation of bone formation through evolution.[2] One mechanism of sclerostin action is via direct antagonism of the Wnt/β-catenin pathway, resulting in inhibition of osteoblast formation and differentiation from precursor cells.[3] Sclerostin may also act as an antagonist of bone morphogenetic proteins.[4] The expression of sclerostin is largely restricted to osteocytes, therefore, its effects are largely selective to skeletal tissue.[5,6]

It has recently been reported that inhibition of sclerostin with a neutralizing sclerostin antibody (Scl-Ab) increased bone formation and restored bone mass and bone strength in the osteopenic, ovariectomized (OVX) rat model.[7] Scl-Ab was also shown to prevent bone loss associated with limb disuse in rats.[8] In addition, Scl-Ab treatment has led to increases in bone formation, bone mass, and bone strength in aged male rats and in nonhuman primate models.[9,10] Similarly, it was reported that Scl-Ab significantly increased bone formation markers and bone mineral density (BMD), and significantly decreased bone resorption markers after a single injection in healthy men and post-menopausal women.[11]

Correspondence to: David G. Little (T: +612-9845-0017; F: +612-9845-3078; E-mail: davidl3@chw.edu.au)

In addition to its efficacy in preclinical models of osteoporosis, Scl-Ab treatment has been reported to enhance fracture healing in intact rats and nonhuman primate models.[12] Further, enhancement of bone healing leading to increased pull-out strength at orthopedic implant sites was observed with Scl-Ab treatment.[13]

It has been noted that compromised bone repair is associated with osteoporosis in elderly patients,[14] and compromised repair in OVX rats is a common observation.[15–17] A number of studies have also begun to address potential therapeutic applications to improve repair in this setting.[18–22] As the majority of osteoporotic fractures occur at the metaphyseal regions due to more extreme bone loss,[23,24] we sought to examine the effect of Scl-Ab on bone repair in OVX rats using a tibial metaphyseal defect repair model. In contrast to diaphyseal bone, which heals indirectly through periosteal callus formation and endochondral bone formation, metaphyseal bone commonly heals directly through intramembranous ossification and endosteal bridging without a significant periosteal callus.

We hypothesized that metaphyseal defect healing would be compromised in OVX rats compared to Sham rats. Additionally, we hypothesized that Scl-Ab treatment would enhance healing of metaphyseal defects in OVX rats via enhanced stimulation of bone formation.

METHODS

Animals and Surgery

OVX or sham surgery was performed in female Sprague Dawley rats and early stage osteopenia was allowed to develop for 4 weeks post-surgery. Dual energy X-ray absorptiometry (DEXA) scans were performed to assess vertebral BMD at L3–L4 and defect surgery was performed in a total of 66

Sham and 66 OVX rats. Bilateral 3 mm circular metaphyseal defects were created in the proximal tibia centered 5 mm from the growth plate [25] using a jig reference system. Radiographs were taken post-defect production (Faxitron MX20, Lincolnshire, IL) to assess correct placement of the defect and to assess for intact cortices. Five rats were culled at surgery due to poor defect placement or fracture of cortices. Samples sizes ranged between 9 and 11 samples per group after exclusions. Post-defect surgery, a ratized sclerostin monoclonal antibody (Scl-AbIII, Amgen Inc., Thousand Oaks, CA) or Saline was administered subcutaneously twice weekly at 25 mg/kg. Calcein (10 mg/kg) was given by subcutaneous injection at 10 and 3 days prior to harvest for assessment of bone formation parameters. At 1, 2, and 3 weeks post-defect surgery, both tibiae and femora were harvested for analysis, fixed in 4% paraformaldehyde at room temperature for 5 h then overnight at 4°C before being transferred to 70% alcohol for storage at 4°C.

Radiographic Analysis

DEXA scans were performed using the Lunar PIXImus scanner (GE-Lunar, Madison, WI) at the time of OVX or sham surgery on all rats to determine vertebral BMD changes at L3–L4 subsequent to OVX. Radiographs were used to visualise healing at harvest time points. Micro-CT (μCT) scans of the entire proximal right tibiae were performed using the SkyScan 1174 system (SkyScan NV, Kontich, Belgium). The defect region was examined using the accompanying CTAn software to determine three-dimensional (3D) bone volume/total volume ratio (BV/TV), bone surface (BS), trabecular number (TbN), and trabecular thickness (TbTh) within the defect, as well as to generate 3D models. The entire defect was examined using 150 slices to encompass the full width of the defect and a 3 mm cross sectional diameter circle region of interest (ROI) (Fig. 1a). The defect was also examined using ROIs placed either on the endosteal surface of the defect cortex or external to the cortical defect (Fig. 1b). This creation of two distinct ROIs was aimed at assessing bone repair driven by metaphyseal/endosteal repair (Endosteal ROI) and cortical/periosteal driven repair (external ROI). One hundred slices were examined within each of these ROIs for each sample. In addition to μCT analysis of the defects, peripheral quantitative computed tomography (pQCT) scans were performed using the Stratec XCT scanner (Stratec Medizintechnik, Pforzheim, Germany) with a slice thickness of 1 mm on the right femora of all rats with four slices in the distal metaphysis and four slices in the mid diaphysis. This facilitated analysis of systemic effects of Scl-Ab in OVX rats in metaphyseal and cortical bone.

Histological Analysis

Left tibiae were decalcified in a solution of 12.5% EDTA and 0.5% PFA at 4°C for 3 days then in 0.34 M EDTA at 4°C for 3–4 weeks and processed to paraffin wax. Central 5 μm sections in the sagittal plane were cut including the 3 mm defect between the cortical edges, similar to the region examined in μCT scans shown in Figure 1b. Sections were stained using haematoxylin eosin for basic morphology and TRAP stain to examine osteoclast morphology and number. The defect area was examined for TRAP-positive cells in two regions: (1) within the center of the healing defect and (2) at the cortical edge (between the two cortical ends) of the defect. Right tibiae were processed undecalcified to resin and sectioned at 5 μm thickness in the same plane as paraffin sections. von Kossa staining was used to measure 2D BV/TV within the defect region and fluorescent microscopy was used to measure the area of labeled bone within the defect using calcein labeling.

Statistical Analysis

All data were analyzed using SPSS with one-way ANOVA and post-hoc *t*-tests using the least squared differences method. Some histological samples could not be processed resulting in an $N < 10$. In these cases a non-parametric test (Mann–Whitney) was used.

RESULTS

Radiographic Outcomes

DEXA scans revealed 9–10% reductions in vertebral BMD in OVX rats compared with Sham rats at 1, 2, and 3 weeks post-defect surgery (data not shown; $p < 0.01$). Radiographs revealed progressive healing of the defect over the time course of the study, with reduced radiodensity in OVX rats but enhanced radiodensity in samples from Scl-Ab-treated rats both

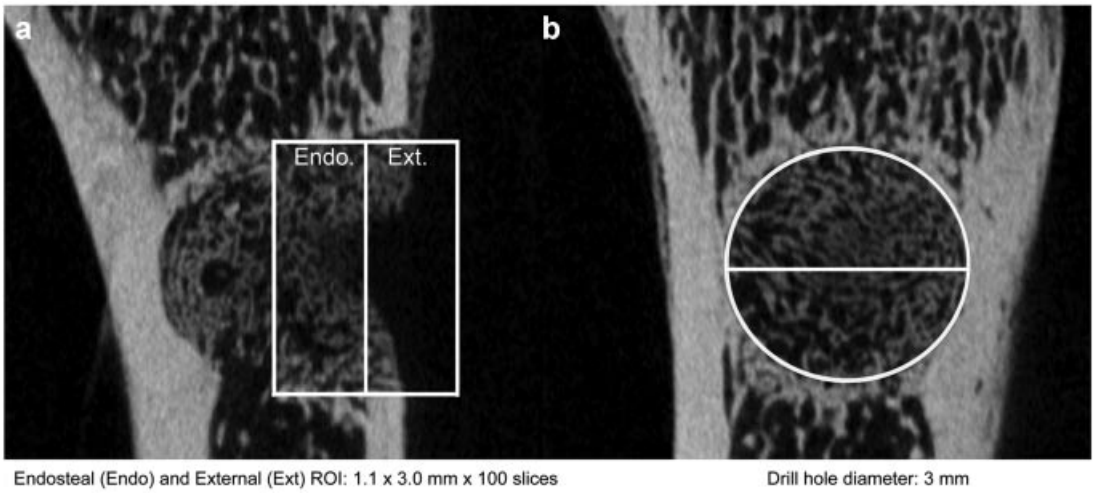

Figure 1. μCT images showing analysis using the following ROIs: (a) external (Ext.) and endosteal (Endo.) ROIs at the cortical edge of the defect with slices aligned in a transaxial plane. (b) entire defect cylinder.

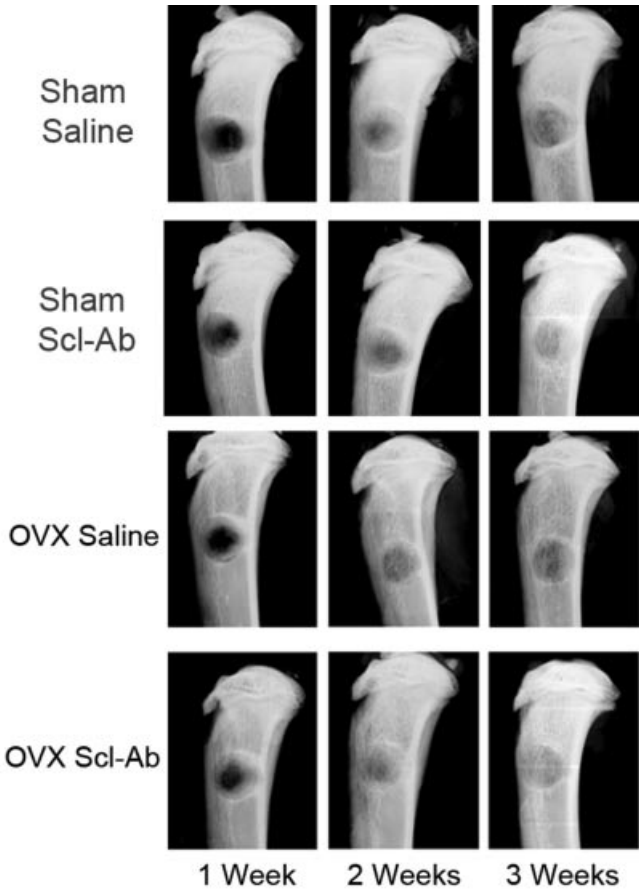

Figure 2. Representative X-rays at 1, 2, and 3 weeks for all treatment groups. Note the increased radio density in Scl-Ab-treated samples.

within and surrounding the defect compared with Saline (Fig. 2).

MicroCT Results of the Entire Defect

μCT analysis of the entire defect of all samples demonstrated significant alterations in bone volume and architecture in response to OVX along with augmentation of repair with Scl-Ab treatment (Fig. 3a–c). A 52% increase in 3D BV/TV was noted at 1-week post-defect surgery in the OVX Saline group compared with the Sham Saline group ($p < 0.05$). However, by 2 weeks, there was a 37% decrease in 3D BV/TV between OVX and Sham Saline groups and by 3 weeks, the difference increased to 44% ($p < 0.01$, Fig. 3a). When considering each group over the 3-week time period, although OVX produced a stronger initial response to healing, the increase in 3D BV/TV between 1 and 2 weeks in OVX Saline was only 129% compared to an increase of 453% in Sham Saline ($p < 0.01$). Further the OVX Saline group showed a 15% decrease in 3D BV/TV between 2 and 3 weeks ($p < 0.05$), Sham Saline plateuing from 2 to 3 weeks. Scl-Ab treatment protected the repairing defect in OVX rats, improving the response from 1 to 2 weeks to an increase of 237% in the Scl-Ab treated OVX rats ($p < 0.01$) such that a 33% increase in 3D BV/TV was noted between Saline OVX and Scl-Ab treated OVX rats at 3 weeks ($p < 0.05$). Further Scl-Ab treatment prevented the loss of bone volume in the defect of OVX rats between 2 and 3 weeks, with no change in BV/TV between these two time points in the Scl-Ab OVX group. Scl-Ab treatment in Sham treated rats however had no significant effect on 3D BV/TV when examining the entire repairing defect. The increased 3D BV/TV in the OVX Scl-Ab samples compared to Sham Saline at 3 weeks was associated with a 35% increase in TbN ($p < 0.01$), with no change in TbTh (Fig. 3b and c).

MicroCT Results of Endosteal/Metaphyseal Driven Repair

When examining the defect in discreet regions, as outlined in Figure 1, within the endosteal ROI (Figs. 1b and 3d–f) we saw interesting alterations in response to OVX with a 43% increase in 3D BV/TV in this region at 1 week in OVX Saline samples compared with Sham Saline ($p < 0.05$, Fig. 3d). Interestingly when examining OVX Saline groups over the 3-week healing period, although the initial response to repair was stronger than Sham, we saw no change in 3D BV/TV between the 1- and 2-week time points, followed by a large reduction of 73% between 2 and 3 weeks ($p < 0.01$). Alternatively, Sham Saline rats, which demonstrated a smaller initial response to injury than OVX at the 1-week time point, actually led to a 300% increase in 3D BV/TV between 1 and 2 weeks, with a small but significant 30% decrease from 2 to 3 weeks ($p < 0.01$). Clearly the healing response in this region of this model is greatly modified by OVX, such that at the 2- and 3-week time points 3D BVTV in OVX Saline samples was reduced by 63% and 86%, respectively compared to Sham Saline ($p < 0.01$). Importantly, Scl-Ab treatment demonstrated strong protective effects in OVX rats. Although no differences were observed between OVX Saline and Scl-Ab-treated OVX samples at the 1- and 2-week time points in this region, by 3 weeks, Scl-Ab treatment in OVX rats increased 3D BV/TV by 200% compared with OVX Saline ($p < 0.05$). In addition, although not evident when examining the entire defect, Scl-Ab treatment in Sham rats did alter repair such that the 30% reduction in 3D BV/TV from 2 to 3 weeks at this endosteal site in Sham Saline rats was prevented and instead a 32% increase in 3D BV/TV was noted between Sham Scl-Ab and Sham Saline at 3 weeks ($p < 0.05$).

While slight alterations in TbTh were seen (Fig. 3f), differences in TbN were the main mechanism for the shifts in 3D BV/TV with Scl-Ab treatment. At 3 weeks, OVX Saline samples showed an 85% reduction in TbN compared with Sham Saline ($p < 0.01$). Scl-Ab treatment, however, attenuated this, such that TbN was increased, by 183% in OVX rats ($p < 0.01$, Fig. 3e).

MicroCT Results of External/Cortical Driven Repair

Interestingly, over the 3-week time period, we saw a more similar pattern of repair between Sham and OVX in this region, with OVX samples showing increased 3D BV/TV compared to Sham Saline at both 1 and 2 weeks, but reaching equivalence with Sham

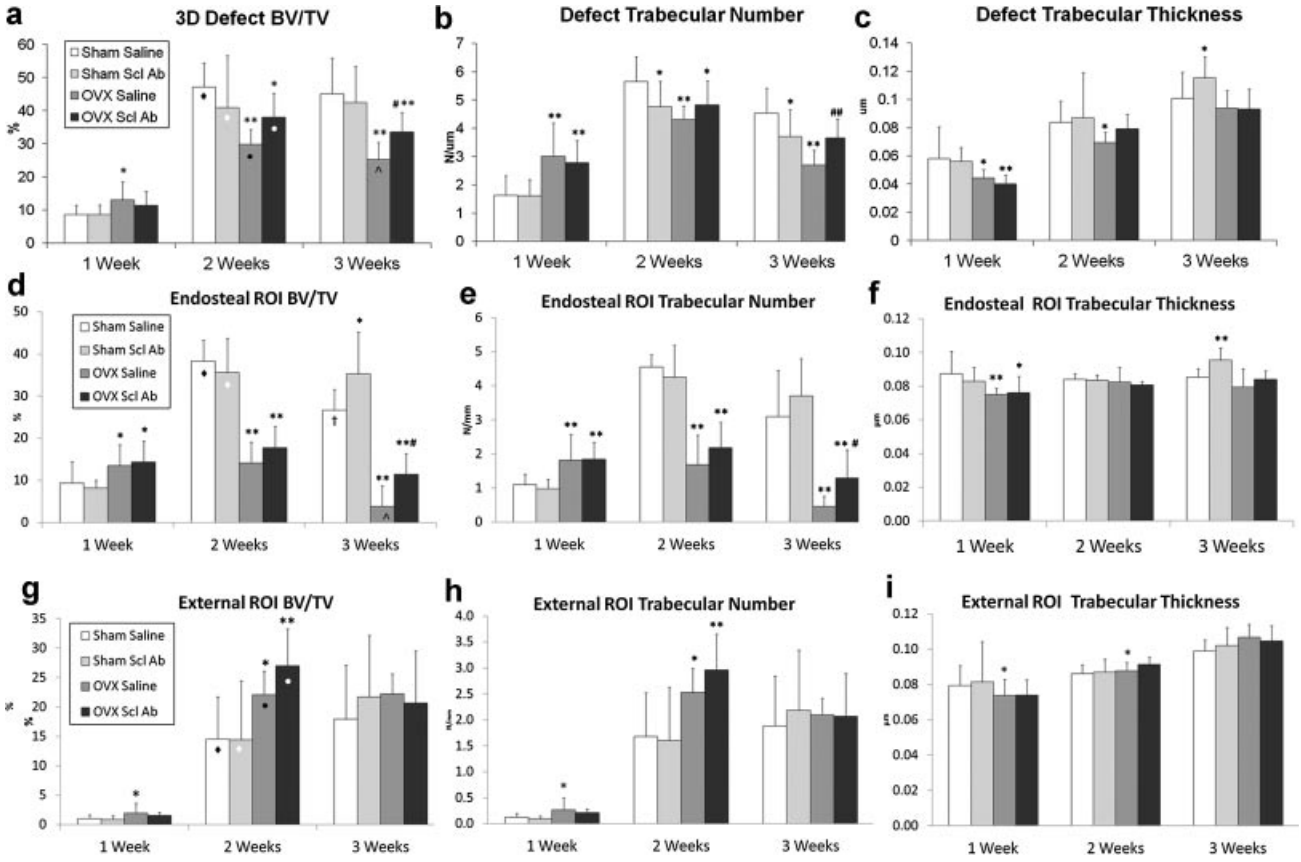

Figure 3. (a–c) Bar charts from MicroCT analysis of the entire defect showing mean 3D bone volume/total volume (a), trabecular number (b), and trabecular thickness (c). (d–f) Bar charts from MicroCT analysis of the endosteal/metaphyseal ROI of the defect showing mean 3D bone volume/total volume (d), trabecular number (e), and trabecular thickness (f). (g–i) Bar charts from MicroCT analysis of the external/cortical ROI of the defect showing mean 3D bone volume/total volume (g), trabecular number (h), and trabecular thickness (i). $^{*}p < 0.05$ compared with Sham Saline, $^{**}p < 0.01$ compared with Sham Saline, $^{\#}p < 0.05$ compared with OVX Saline, $^{\#\#}p < 0.01$ compared with OVX Saline. $^{\blacklozenge}p < 0.01$ compared with Sham Saline 1 week, $^{\blacksquare}p < 0.01$ compared with Sham Scl-Ab 1 week, $^{\bullet}p < 0.01$ compared with OVX Saline 1 week, $^{\blacksquare}p < 0.01$ compared with OVX Scl-Ab 1 week, $^{\wedge}p < 0.05$ compared with OVX Saline 2 weeks, $^{\dagger}p < 0.01$ compared with Sham Saline 2 weeks.

Saline by 3 weeks (Fig. 3g–i). Scl-Ab treatment did not produce significant changes in this region in either sham or OVX rats.

Systemic Effects of Scl-Ab

Systemic effects of Scl-Ab in OVX animals were confirmed, with a 4% increase in cortical BMD and a 7% increase in metaphyseal BMD noted after 3 weeks of Scl-Ab treatment compared with OVX Saline ($p < 0.05$; data not shown). Metaphyseal BMD was also increased by 4% in Sham Scl-Ab treated rats compared to Sham Saline ($p < 0.05$; data not shown).

Histological Analysis

BV/TV

Histological assessment of the entire defect on one representative central section confirmed the findings of our μCT data from the entire defect. The intial response to injury at 1 week was enhanced in response to OVX with a 157% increase in BV/TV compared with Sham Saline ($p < 0.01$, Table 1, Fig. 4). Between 1–2 and 2–3 weeks however, OVX Saline showed a trend for reduced BV/TV in contrast to sham Saline samples which demonstrated an increase of over threefold in BV/TV from 1 to 2 weeks ($p < 0.01$) and no change from 2 to 3 weeks. As a result, BV/TV in OVX Saline samples was reduced by 45% at 2 weeks and 53% at 3 weeks compared with Sham Saline samples ($p < 0.01$). As demonstrated radiologically, Scl-Ab treatment atenuated this impaired healing in OVX rats, with a strong 36% increase in BV/TV from 1 to 2 weeks, leading to an overall increase in BV/TV of 63% at 2 weeks ($p < 0.01$) and 38% at 3 weeks ($p < 0.02$) compared to Saline OVX. Further, Scl-Ab treatment in Sham rats revealed a 24% increase in BV/TV at 3 weeks compared to Sham Saline ($p = 0.06$). Histologically, both TbTh and TbN were increased with Scl-Ab treatment ($p < 0.05$, Table 1, Fig. 4).

Bone Formation

Analysis of the area of fluorescently labeled bone in the defect showed enhanced labeled bone area in Scl-Ab-treated samples (Fig. 5). Scl-Ab treatment at 2 weeks produced a 61% increase in labelled bone area compared with OVX Saline ($p < 0.05$), and an 80% increase at 3 weeks, although this was not significant.

Table 1. Histological Analysis Data from the Entire Defect Region

		1 Week				2 Weeks				3 Weeks			
Parameter	Units	Sham Saline	Sham Scl-Ab	OVX Saline	OVX Scl-Ab	Sham Saline	Sham Scl-Ab	OVX Saline	OVX Scl-Ab	Sham Saline	Sham Scl-Ab	OVX Saline	OVX Scl-Ab
BV/TV	%	8.3 (4.9)	8.5 (6.3)	21.3** (14.3)	18.6* (8.6)	28.0 (5.5)	32.0 (7.9)	15.5** (5.2)	25.3$^{\#\#}$ (7.4)	28.9 (11.0)	35.8† (7.9)	13.7** (3.4)	18.9$^{*\,\#}$ (9.2)
TbN	N/mm	1.37 (0.73)	1.52 (0.91)	2.84** (1.15)	2.87* (0.86)	3.30 (0.47)	3.30 (0.57)	1.72** (0.50)	2.40$^{\#\#\,**}$ (0.53)	2.02 (0.61)	2.16 (0.46)	0.88** (0.23)	1.09** (0.48)
TbTh	μm^2	58.3 (9.15)	53.5 (9.39)	69.8 (27.2)	63.0 (11.3)	84.6 (9.1)	96.1 (10.5)	89.5 (12.1)	105.3** (18.7)	148.9 (64.3)	169.8 (40.5)	168.6 (77.2)	199.1 (95.9)
OcN/BS center	N/mm	—	—	—	—	0.004 (0.001)	0.002** (0.001)	0.002** (0.001)	0.002 (0.001)	0.002 (0.001)	0.002 (0.001)	0.002 (0.001)	0.002 (0.001)
OcN/BS cortical	N/mm	—	—	—	—	0.004 (0.001)	0.002** (0.001)	0.003 (0.001)	0.003 (0.001)	0.002 (0.001)	0.002 (0.001)	0.001* (0.001)	0.002 (0.001)

$^{*}p < 0.05$ compared to Sham Saline. $^{**}p < 0.01$ compared to Sham Saline. $^{\#}p < 0.05$ compared to OVX Saline. $^{\#\#}p < 0.01$ compared to OVX Saline. $^{\dagger}p = 0.06$ compared to Sham Saline.

Figure 4. Representative von kossa-stained sections of proximal tibia including the defect in a transaxial plane (similar plane to Fig. 1b). Note the decreased bone volume/total volume in OVX Saline compared with Sham Saline samples at 2 and 3 weeks. Also note the effects of Scl-Ab treatment in OVX samples with increased BV/TV at 2 and 3 weeks and in sham samples increased by 3 weeks.

Again altered repair was noted in OVX Saline treated rats, with the peak of labeled bone area shown at 1 week in OVX, decreasing steadily to 3 weeks. In contrast to Sham Saline rats which peaked at 2 weeks before reducing slilghtly to 3 weeks. As a result by 3 weeks, OVX Saline rats showed a 54% decrease in labeled bone area compared to Sham Saline ($p < 0.05$). Scl-Ab clearly attenuated this impaired healing in OVX rats with a strong increase in labeled bone area to 2 weeks and no reduction to 3 weeks, a more similar pattern to Sham Saline samples. This was such that Scl-Ab OVX group was equivalent to Sham Saline in laballed bone area by 3 weeks. Scl-Ab treatment in sham rats did not significantly alter labeled bone area (Fig. 5).

Bone Resorption

The number of TRAP-positive cells per unit of BS (OscN/BS) was not significantly altered with Scl-Ab treatment in OVX rats (Table 1). However, differences were detected between samples from OVX and Sham rats. At 2 weeks, OVX Saline samples showed a 36% reduction in osteoclast number per unit bone surface

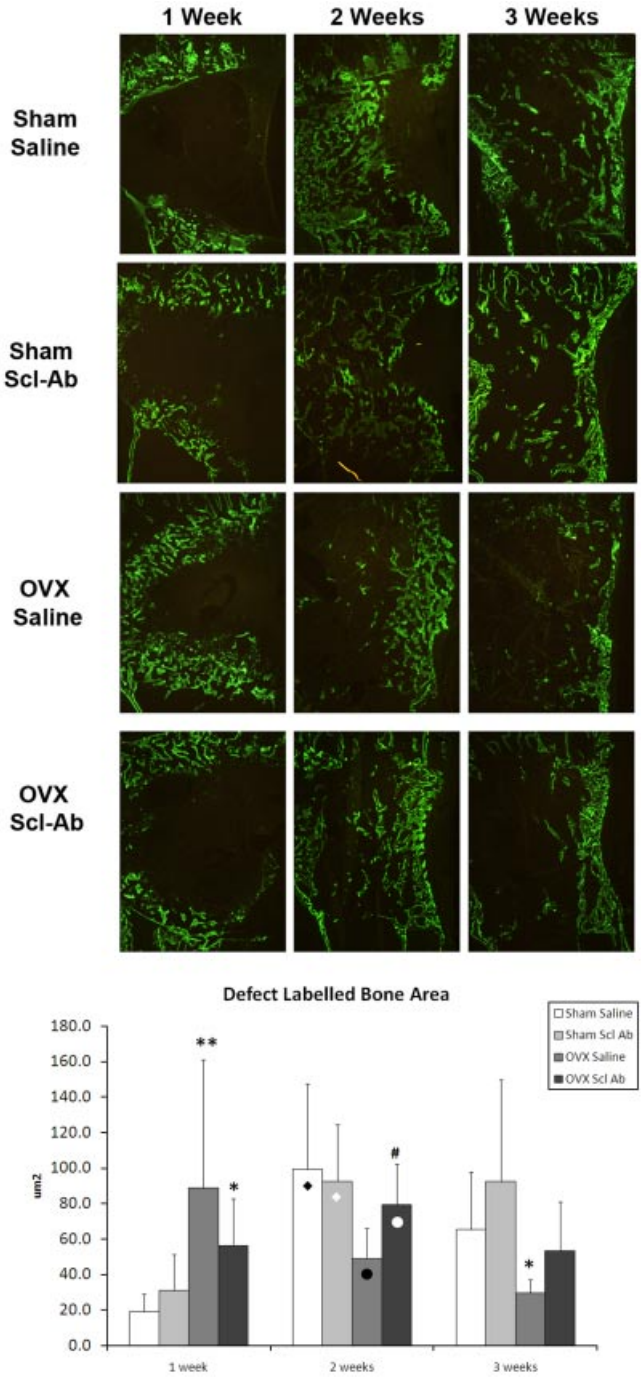

Figure 5. (a) Representative images of sections of the defect area labeled with calcein (green) at 10 and 7 days prior to cull at each time point. Note the corresponding increases in labelled bone surfaces to the von kossa stained images in Figure 4. Scl-Ab treatment significantly increased labelled bone area at 2 weeks but the 3-week increase was not significant. (b) Bar chart of mean labelled bone area. Error bars are 1 SD. $^{*}p < 0.05$ compared with Sham Saline, $^{**}p < 0.01$ compared with Sham Saline, $^{\#}p < 0.05$ compared with OVX Saline. $^{\blacklozenge}p < 0.01$ compared with Sham Saline 1 week, $p < 0.01$ compared with Sham Scl-Ab 1 week, $^{\bullet}p < 0.01$ compared with OVX Saline 1 week, $p < 0.01$ compared with OVX Scl-Ab 1 week. [Color figure can be seen in the online version of this article, available at http://wileyonlinelibrary.com/journal/jor]

(OcN/BS; $p < 0.01$) in the center of the defect compared with Sham Saline, followed by normalisation to sham levels at 3 weeks. At 3 weeks however, OVX Saline samples showed a 53% reduction in OcN/BS compared with Sham Saline at the cortical edge of the defect ($p < 0.05$). Interestingly at 2 weeks Scl-Ab treatment in sham rats reduced OcN/BS by 43% compared to Saline sham both in the center of the defect and at the cortical edge in sham rats ($p < 0.01$). At 1 week, very few TRAP-positive cells were noted in any samples so no measurements were possible.

DISCUSSION

Bone repair in this metaphyseal defect model was significantly compromised in OVX animals compared to sham, however Scl-Ab treatment improved repair outcomes in OVX rats, largely normalizing the repair response. Impaired bone healing in OVX rats is consistent with numerous previous studies describing impaired endochondral bone repair in this osteoporotic animal model induced by estrogen deficiency.[15–17] Of interest, our detailed assessment of the metaphyseal intramembranous repair model revealed an alteration in the repair response in OVX rats. Acceleration of the initial response to injury was noted in OVX Saline-treated rats, with increases of up to 157% in 2D BV/TV, 116% in 3D BV/TV and increases of over 300% in defect-labeled bone area compared to sham Saline samples at the early 1-week time point. From this stage onwards however bone formation reduced steadily in OVX rats such that the resultant bone volume fell significantly behind Sham Saline-treated animals at both 2 and 3 weeks on the endosteal surface of the defect (Fig. 3). We suggest that the early enhanced response in OVX rats is due to accelerated bone turnover in this region. As shown in previous studies of both the distal femur[26,27] and the proximal tibia,[28] metaphyseal bone turnover is extremely high in the early stages post-OVX. Although our analysis of osteoclast number/bone surface suggested OVX rats had reduced resorption at 2 and 3 weeks, the overall impaired healing response led to a net decrease in bone volume within the defect of OVX rats compared to Sham. Even though a number of other studies have explored metaphyseal fracture repair in OVX animals, data to compare with our interesting finding of early enhanced bone formation is lacking[29–32]. Further to this, the bone repair process at the periosteal/cortical edge of the defect was not impaired with OVX, instead it was either equivalent to or increased compared to sham. These different outcomes indicate that OVX influences metaphyseal bone repair differently to cortical bone in this defect model, a result that may require further assessment to understand completely.

Treatment with Scl-Ab, during healing in the current bone repair model, increased considerably the amount of bone formed at the endosteal region of the repair site during the later stages in OVX rats, leading

to normalization of the repair response. The accelerated repair reaction at 1 week in OVX rats, with peak bone formation at this early stage, was in fact followed by impaired bone formation and resultant reduced bone volume in this region of the repair site compared to sham controls. Scl-Ab treatment prevented the reduction in bone formation in OVX rats, instead increasing labeled bone area from 1 to 2 weeks, reaching Sham Saline levels by the 3-week time point. As a result, defect bone volume was augmented significantly, in OVX samples with Scl-Ab treatment at 2 and 3 weeks, virtually normalizing with Sham Saline levels by 3 weeks. Analysis at a later time point, 4 or 5 weeks, would be needed to confirm complete normalization of OVX defect repair to sham levels through Scl-Ab treatment. Enhancement of healing with Scl-Ab treatment in sham rats was also documented in this study, although not to the extent of that seen in OVX rats. Interestingly, based on our histological assessment, this may be attributed to reduced bone resorption rather than the enhanced bone formation documented in Scl-Ab treated OVX rats.

Improvement of impaired healing in OVX rats has been demonstrated previously through the use of either raloxifene or estrogen in a metaphyseal osteotomy model.[30] Interestingly, the anti-resorptive agent, alendronate, failed to improve mechanical properties in metaphyseal healing in this model,[31] with conflicting previous reports in OVX diaphyseal fractures.[19,20]

More promising than these other agents is the strong augmentation of bone repair through use of Scl-Ab showing improved fracture union rate, increased bone formation, enhanced callus size, and superior mechanical strength in non-impaired models of bone healing.[12,13] Our current data confirms these findings with enhanced bone formation, bone volume and hence improved intramembranous defect repair in Scl-Ab-treated OVX rats. Although our model involves intramembranous repair only, this work suggests that Scl-Ab treatment in diaphyseal repair models, which encompass both endochondral and intramembranous repair, may be enhanced on two levels with both these modes of bone formation augmented. With its powerful bone-specific anabolic activity, and potentially low dosing frequency regime in humans,[11] Scl-Ab treatment may provide a novel avenue for investigations into the enhancement of both endochondral and intramembranous bone repair. This is particularly relevant in situations of compromised bone repair such as osteoporosis.

ACKNOWLEDGMENTS

Funding for the study was provided by Amgen Inc. and UCB. Michelle N. Bradley, PhD, provided editorial support on behalf of Amgen Inc. Min Liu and Hua Zhu Ke are Amgen Inc. employees and own Amgen Inc. stock and/or stock options.

REFERENCES

1. Balemans W, Ebeling M, Patel N, et al. 2001. Increased bone density in sclerosteosis is due to the deficiency of a novel secreted protein (SOST). Hum Mol Genet 10:537–543.
2. Li X, Ominsky MS, Niu QT, et al. 2008. Targeted deletion of the sclerostin gene in mice results in increased bone formation and bone strength. J Bone Miner Res 23:860–869.
3. Li X, Zhang Y, Kang H, et al. 2005. Sclerostin binds to LRP5/6 and antagonizes canonical Wnt signaling. J Biol Chem 280:19883–19887.
4. Krause C, Korchynskyi O, de Rooij K, et al. 2010. Distinct modes of inhibition by sclerostin on bone morphogenetic protein and wnt signaling pathways. J Biol Chem 285:41614–41626.
5. Winkler DG, Sutherland MK, Geoghegan JC, et al. 2003. Osteocyte control of bone formation via sclerostin, a novel BMP antagonist. EMBO J 22:6267–6276.
6. Poole KE, van Bezooijen RL, Loveridge N, et al. 2005. Sclerostin is a delayed secreted product of osteocytes that inhibits bone formation. FASEB J 19:1842–1844.
7. Li X, Ominsky MS, Warmington KS, et al. 2009. Sclerostin antibody treatment increases bone formation, bone mass and bone strength in a rat model of postmenopausal osteoporosis. J Bone Miner Res 24:578–588.
8. Tian X, Jee WS, Li X, et al. 2011. Sclerostin antibody increases bone mass by stimulating bone formation and inhibiting bone resorption in a hindlimb-immobilization rat model. Bone 48:197–201.
9. Li X, Warmington KS, Niu QT, et al. 2010. Inhibition of sclerostin by monoclonal antibody increases bone formation, bone mass, and bone strength in aged male rats. J Bone Miner Res 25:2371–2380.
10. Ominsky MS, Vlasseros F, Jolette J, et al. 2010. Two doses of sclerostin antibody in cynomolgus monkeys increases bone formation, bone mineral density, and bone strength. J Bone Miner Res 25:948–959.
11. Padhi D, Jang G, Stouch B, et al. 2011. Single-dose, placebo-controlled, randomized study of AMG 785, a sclerostin monoclonal antibody. J Bone Miner Res 26:19–26.
12. Ominsky MS, Li C, Li X, et al. 2011. Inhibition of sclerostin by monoclonal antibody enhances bone healing and improves bone density and strength of non-fractured bones. J Bone Miner Res 26:1012–1021.
13. Agholme F, Li X, Isaksson H, et al. 2010. Sclerostin antibody treatment enhances metaphyseal bone healing in rats. J Bone Miner Res 25:2412–2418.
14. Barrios C, Broström LA, Stark A, et al. 1993. Healing complications after internal fixation of trochanteric hip fractures: the prognostic value of osteoporosis. J Orthop Trauma 7:438–442.
15. Kubo T, Shiga T, Hashimoto J, et al. 1999. Osteoporosis influences the late period of fracture healing in a rat model prepared by ovariectomy and low calcium diet. J Steroid Biochem Mol Biol 68:197–202.
16. Namkung-Matthai H, Appleyard R, Jansen J, et al. 2001. Osteoporosis influences the early period of fracture healing in a rat osteoporotic model. Bone 28:80–86.
17. Augat P, Simon U, Liedert A, et al. 2005. Mechanics and mechanobiology of fracture healing in normal and osteoporotic bone. Osteoporos Int 16:S36–S43.
18. Shuid AN, Mohamad S, Mohamed N, et al. 2010. Effects of calcium supplements on fracture healing in a rat osteoporotic model. J Orthop Res 28:1651–1656.
19. Cao Y, Mori S, Mashiba T, et al. 2002. Raloxifene, estrogen, and alendronate affect the processes of fracture repair differently in ovariectomized rats. J Bone Miner Res 17:2237–2246.
20. Saito M, Shiraishi A, Ito M, et al. 2010. Comparison of effects of alfacalcidol and alendronate on mechanical properties and bone collagen cross-links of callus in the fracture repair rat model. Bone 46:1170–1179.

21. Fu L, Tang T, Miao Y, et al. 2009. Effect of 1,25-dihydroxy vitamin D3 on fracture healing and bone remodeling in ovariectomized rat femora. Bone 44:893–898.
22. Habermann B, Kafchitsas K, Olender G, et al. 2010. Strontium ranelate enhances callus strength more than PTH 1–34 in an osteoporotic rat model of fracture healing. Calcif Tissue Int 86:82–89.
23. van der Linden JC, Homminga J, Verhaar JA, et al. 2001. Mechanical consequences of bone loss in cancellous bone. J Bone Miner Res 16:457–465.
24. Peng Z, Tuukkanen J, Zhang H, et al. 1994. The mechanical strength of bone in different rat models of experimental osteoporosis. Bone 15:523–532.
25. Le Guehennec L, Goyenvalle E, Aguado E, et al. 2005. Small-animal models for testing macroporous ceramic bone substitutes. J Biomed Mater Res B Appl Biomater 72: 69–78.
26. Baldock PA, Morris HA, Need AG, et al. 1998. Variation in the short-term changes in bone cell activity in three regions of the distal femur immediately following ovariectomy. J Bone Miner Res 13:1451–1457.
27. Sims NA, Morris HA, Moore RJ, et al. 1996. Increased bone resorption precedes increased bone formation in the ovariectomized rat. Calcif Tissue Int 59:121–127.
28. Wronski TJ, Dann LM, Scott KS, et al. 1989. Long-term effects of ovariectomy and aging on the rat skeleton. Calcif Tissue Int 45:360–366.
29. Kolios L, Sehmisch S, Daub F, et al. 2009. Equol but not genistein improves early metaphyseal fracture healing in osteoporotic rats. Planta Med 75:459–465.
30. Stuermer EK, Sehmisch S, Rack T, et al. 2010. Estrogen and raloxifene improve metaphyseal fracture healing in the early phase of osteoporosis. A new fracture-healing model at the tibia in rat. Langenbecks Arch Surg 395:163–172.
31. Kolios L, Hoerster AK, Sehmisch S, et al. 2010. Do estrogen and alendronate improve metaphyseal fracture healing when applied as osteoporosis prophylaxis? Calcif Tissue Int 86:23–32.
32. Kolios L, Schumann J, Sehmisch S, et al. 2010. Effects of black cohosh (*Cimicifuga racemosa*) and estrogen on metaphyseal fracture healing in the early stage of osteoporosis in ovariectomized rats. Planta Med 76:850–857.